Tree Physiology 37, 301–315
doi:10.1093/treephys/tpw117

Research paper

Thermotolerance and heat stress responses of Douglas-fir and ponderosa pine seedling populations from contrasting climates

Danielle E. Marias[1,4], Frederick C. Meinzer[2], David R. Woodruff[2] and Katherine A. McCulloh[3]

[1]Department of Forest Ecosystems and Society, Oregon State University, Corvallis, OR 97331, USA; [2]USDA Forest Service, Pacific Northwest Research Station, 3200 SW Jefferson Way, Corvallis, OR 97331, USA; [3]Department of Botany, University of Wisconsin-Madison, Madison, WI 53705, USA; [4]Corresponding author (danielle.marias@oregonstate.edu)

Received September 7, 2016; accepted November 7, 2016; published online December 22, 2016; handling Editor David Tissue

Temperature and the frequency and intensity of heat waves are predicted to increase throughout the 21st century. Germinant seedlings are expected to be particularly vulnerable to heat stress because they are in the boundary layer close to the soil surface where intense heating occurs in open habitats. We quantified leaf thermotolerance and whole-plant physiological responses to heat stress in first-year germinant seedlings in two populations each of *Pinus ponderosa* P. and C. Lawson (PIPO) and *Pseudotsuga menziesii* (Mirb.) Franco (PSME) from climates with contrasting precipitation and temperature regimes. Thermotolerance of detached needles was evaluated using chlorophyll fluorescence (F_V/F_M, F_O) and electrolyte leakage. PSME was more heat tolerant than PIPO according to both independent assessments of thermotolerance. Following exposure of whole seedlings to a simulated heat wave at 45 °C for 1 h in a growth chamber, we monitored F_V/F_M, photosynthesis, stomatal conductance, non-structural carbohydrates (NSCs) and carbon isotope ratios ($\delta^{13}C$) for 14 days. Heat treatment induced significant reductions in F_V/F_M in both species and a transient reduction in photosynthetic gas exchange only in PIPO 1 day after treatment. Heat treatment induced an increase in glucose + fructose concurrent with a decrease in starch in both species, whereas total NSC and sucrose were not affected by heat treatment. The negative relationship between glucose + fructose and starch observed in treated plants may be due to the conversion of starch to glucose + fructose to aid recovery from heat-induced damage. Populations from drier sites displayed greater $\delta^{13}C$ values than those from wetter sites, consistent with higher intrinsic water-use efficiency and drought resistance of populations from drier climates. Thermotolerance and heat stress responses appeared to be phenotypically plastic and representative of the environment in which plants were grown, whereas intrinsic water-use efficiency appeared to reflect ecotypic differentiation and the climate of origin.

Keywords: carbon isotope ratios, chlorophyll fluorescence, electrolyte leakage, heat stress, heat tolerance, non-structural carbohydrates, photosynthesis, stomatal conductance.

Introduction

High temperature stress and heat waves are expected to increase in frequency and intensity throughout the 21st century (Intergovernmental Panel on Climate Change 2014). Although temperature is a strong driver of plant species' distributions, the impacts of high temperature and heat stress on plant physiological performance are not fully understood. While heat and drought are closely related, future increases in temperature and heat waves are predicted to occur with and without drought (Hao et al. 2013), emphasizing the need for research that isolates the effect of high temperature stress on physiological processes. Seedlings represent the most vulnerable plant developmental stage because of their high susceptibility to abiotic and biotic stressors. High temperature stress at the soil surface is a major threat to seedling establishment. Kolb and Robberecht (1996) measured air temperatures exceeding 75 °C at 5 mm above the soil surface, and 45 °C at seedling height or 50 mm above the soil surface during two growing seasons where

maximum ambient air temperatures were ~30 °C. Given that soil surface temperatures are expected to increase along with projected increases in ambient air temperature and the frequency of heat waves, characterizing seedling physiological responses to heat stress is crucial.

Heat stress impacts plant function from the cellular to whole-plant scale. High temperatures damage photosystem II (PSII) photochemistry, electron transport, thylakoid and cell membrane fluidity and ribulose bisphosphate carboxylase–oxygenase (RUBISCO) function, and induce reactive oxygen species production (Wahid et al. 2007, Bita and Gerats 2013, Teskey et al. 2015). Heat stress also increases respiration, reduces photosynthesis, stomatal conductance, growth and reproduction, and leads to leaf abscission, visible foliar damage and mortality (Wahid et al. 2007, Bita and Gerats 2013, Teskey et al. 2015). Plants employ mechanisms that influence the ability to withstand and/or avoid heat stress. This includes producing heat shock proteins that desaturate membrane lipids to maintain cell membrane integrity (Horváth et al. 2012), using assimilated carbon to repair heat-induced damage (Sevanto and Dickman 2015), and regulating evaporative cooling to avoid high leaf temperatures (Tomlinson et al. 2013). Quantifying these physiological responses from the cellular to whole-plant scale informs our understanding of heat (high temperature) tolerance or thermotolerance and mechanisms to cope with heat stress.

Although increased allocation of assimilated carbon (i.e., photosynthate) to repair processes may facilitate recovery from heat stress-induced damage (Bita and Gerats 2013), shifts in plant carbon allocation in response to heat stress are poorly understood due to contradictory results (Génard et al. 2008, Sala et al. 2012, Hartmann and Trumbore 2016). Non-structural carbohydrates (NSCs) include starch and free soluble sugars (sucrose, glucose and fructose) and have multiple fates including growth, storage, reproduction, metabolism, root exudation and repair after stress-induced damage (Kozlowski 1992, Dietze et al. 2014). High levels of leaf NSCs have been associated with heat stress tolerance (Liu and Huang 2000, Niinemets 2010) and are used for damage prevention, osmoregulation and sugar signaling (Roitsch and González 2004, Couée et al. 2006, Sugio et al. 2009). Non-structural carbohydrates may be allocated to above-ground tissues for repair from heat stress and leaf NSC levels may increase (Sevanto and Dickman 2015). In contrast, leaf NSCs may decrease in response to heat stress because photosynthesis and stomatal conductance are inhibited, reducing carbon gain and assimilation (i.e., decreased supply). This may occur concurrently with heat-induced increases in respiration, which utilizes carbon (i.e., increased demand) and depletes NSC reserves (Duan et al. 2013, Zhao et al. 2013, Escandón et al. 2016). Heat stress may also induce shifts between NSC pools (e.g., starch, sugars), as well as turnover of NSC that may be reflected in shifts in the carbon isotope ratios of leaves (Gutierrez and Meinzer 1994). Investigating the impacts of heat stress on NSC dynamics will provide insights into the nature of physiological responses to high temperature stress.

Plant responses to heat stress may vary depending on the climate of origin. Species originating from warmer climates are more heat tolerant and are better adapted to withstand heat stress than species originating from cooler climates (Salvucci and Crafts-Brandner 2004, Cunningham and Read 2006). Similar patterns have been observed within a species whose geographic range spans contrasting climate regimes. Populations within a species can acclimate to varying environmental conditions through phenotypic plasticity where the physiological characteristics reflect the climate in which they are grown (Knight and Ackerly 2002, Ghouil et al. 2003, Gimeno et al. 2009). A species can also survive contrasting climate regimes through ecotypic variation that results from genetically distinct populations within a species that have traits representing different ecotypes and climates of origin (Lindgren and Hällgren 1993, Aranda et al. 2009, Ramírez-Valiente et al. 2010, Du et al. 2014, Matías et al. 2016). Kerr et al. (2015) showed strong evidence for the existence of ponderosa pine ecotypes because a seedling population from a dry climate displayed physiological traits associated with greater drought resistance than a population from a mesic climate despite being grown in a common garden. Phenotypic plasticity and ecotypic variation both enable species to survive diverse climates and buffer against predicted changes in temperature. Thus, species adapted to a wide range of climates may have an advantage over narrowly adapted species (Gimeno et al. 2009) in response to the predicted increases in heat stress. Populations and species originating from contrasting climates are expected to exhibit different heat tolerances and associated physiological responses to heat stress.

Pinus ponderosa P. and C. Lawson (PIPO) and *Pseudotsuga menziesii* (Mirb.) Franco (PSME) are ecologically, economically and socially important native species in the northwestern USA. PIPO and PSME have overlapping geographic ranges with both species ranging from British Columbia, Canada to Mexico and from the Pacific coast to the Rocky Mountains (Burns and Hankala 1990). PIPO is found at elevations from sea level to 3050 m (Oliver et al. 1990) and PSME is found at elevations from sea level to 2700 m (Hermann and Lavender 1990). Generally, PIPO is more tolerant of drought, frost, sun and fire than PSME (Hermann and Lavender 1990, Oliver et al. 1990). Populations of both PIPO and PSME originating from contrasting climates have exhibited ecotypic adaptations that reflect the climate of origin (Sorensen 1983, Perić et al. 2009, Du et al. 2014, Kerr et al. 2015). Because drought results in stomatal closure and increased leaf temperatures (Kolb and Robberecht 1996), populations from drier climates are expected to also have greater heat tolerances.

In this study, we evaluated physiological responses to heat stress in greenhouse-grown first-year germinant seedlings in two populations each of PIPO and PSME originating from climates with contrasting precipitation and temperature regimes.

We first quantified heat tolerance of detached needles using two independent methods: chlorophyll fluorescence and electrolyte leakage. We then evaluated whole-plant responses to heat stress in situ by exposing seedlings to a simulated heat wave in a growth chamber and monitoring chlorophyll fluorescence, photosynthesis, stomatal conductance, carbon isotope ratios and NSC dynamics for 14 days after heat exposure. We hypothesized that (i) populations originating from drier climates would display greater homeostasis of physiological properties (chlorophyll fluorescence, photosynthesis, stomatal conductance, intrinsic water-use efficiency as estimated from carbon isotope ratios, and NSC content and composition) indicating greater heat tolerance than those from wetter climates, and (ii) based on stability of the preceding physiological properties, PIPO would display greater heat tolerance than PSME.

Materials and methods

Plant material

Pinus ponderosa P. and C. Lawson (PIPO) and *P. menziesii* (Mirb.) Franco (PSME) seeds were obtained from the Oregon Department of Forestry and the USFS Pacific Northwest Research Station, respectively. Two populations of each species originated from a drier and a wetter climate ($PIPO_{dry}$, $PIPO_{wet}$, $PSME_{dry}$ and $PSME_{wet}$) based on mean annual precipitation (MAP) and temperature for each population within each species (Table 1, PRISM). $PIPO_{dry}$ originated near Spray, OR (44.8343°N, 119.7944°W) on the east side of the Cascade mountains ~325 km from the coast, which has a MAP of 337 mm. $PIPO_{wet}$ originated from the Willamette Valley, OR with climate similar to Corvallis, OR (44.5646 N, 123.2620 W) on the west side of the Cascade mountains ~84 km from the coast, which has a MAP of 1043 mm. $PSME_{dry}$ originated from near Tiller, OR (42.895 N, 123.0 W), which has a MAP of 1056 mm. $PSME_{wet}$ originated from the Coast Range (44.851 N, 123.818 W), which has a MAP of 3054 mm. For clarity, populations were named 'dry' and 'wet' based on relative differences in MAP between each population within each species. Climate information of each population is summarized in Table 1. Seeds were stratified in February of 2014 and planted in 3 l pots with a peat–perlite–pumice growing mix (Sunshine LA4P, Sun Gro Horticulture, Agawam, MA) in a temperature-controlled greenhouse in Corvallis, Oregon in March of 2014. During the sampling campaigns in October and November 2014, seedlings were ~10 cm tall, average daytime temperature in the greenhouse was 22 °C, average nighttime temperature 19 °C, average daytime relative humidity 67% and average daily maximum photosynthetic photon flux density (PPFD) was 285 μmol m^{-2} s^{-1} (see Table S1 available as Supplementary Data at *Tree Physiology* Online). Average daily maximum PPFD was 391 μmol m^{-2} s^{-1} for the growing season from April to September. Seedlings were watered three times per week and fertilized once every 2 weeks (12%N, 4%P_2O_5, 8%K_2O).

Thermotolerance curves derived from chlorophyll fluorescence

During October of 2014, two mature needles were collected from each of five seedlings per population prior to dawn to ensure needles were dark acclimated. Needles were placed in closed plastic bags and immersed in a preheated water bath (General Purpose Aquabath Model 2343, Thermo Fisher Scientific, Marietta, OH, USA) for 15 min at 9 temperatures ranging from 25 to 59 °C for PIPO and 12 temperatures ranging from 25 to 61 °C for PSME. Different sets of needles were exposed to each temperature. A fine-wire thermocouple in each plastic bag recorded that needles reached each desired temperature within 1 min. Chlorophyll fluorescence was measured at room temperature with a portable pulse-amplitude modulated chlorophyll fluorometer (Mini-PAM, Heinz Walz GmbH, Effeltrich, Germany) 24 h after exposure to each temperature. Controls were not exposed to a water bath treatment. During the 24 h after temperature exposure, needles were stored in the dark on moist filter paper in Petri dishes.

Chlorophyll fluorescence was measured as the ratio of variable to maximum fluorescence (F_V/F_M) and the minimal level of fluorescence (F_O) in the convention of Maxwell and Johnson (2000). F_V/F_M is a proxy for the maximum quantum efficiency of PSII photochemistry (Genty et al. 1989) and is calculated as

Table 1. MAP and mean minimum and maximum temperatures in winter (December–February) and summer (June–August) of each PIPO and PSME population.

	$PIPO_{dry}$	$PIPO_{wet}$	$PSME_{dry}$	$PSME_{wet}$
Coordinates	44.8343°N, 119.7944°W	44.5646°N, 123.2620°W	42.895°N, 123.0°W	44.851°N, 123.818°W
Elevation (m)	621	71	750	401
MAP (mm)	337	1043	1056	3054
Winter (Dec.–Feb.)				
Minimum temperature (°C)	−2.7	1.2	0.2	1.5
Maximum temperature (°C)	8.4	8.6	9.1	8.3
Summer (Jun.–Aug.)				
Minimum temperature (°C)	10.7	10.2	10.4	9.2
Maximum temperature (°C)	32.4	25.8	26.9	21.1

$$\frac{F_V}{F_M} = \frac{F_M - F_O}{F_M} = 1 - \frac{F_O}{F_M} \quad (1)$$

F_O was induced by turning on a measuring light (red light-emitting diode, 650 nm, 0.15 μmol m^{-2} s^{-1} PPFD) with a pulse width of 3 μs at a pulse modulation frequency of 0.6 kHz. F_V/F_M was then determined by applying a 0.8-s saturating pulse of white light, which transiently closed all PSII reaction centers, minimized heat dissipation and induced maximum fluorescence, allowing the determination of variable fluorescence. Reductions in F_V/F_M indicate stress-induced changes in photochemistry such as inhibition of PSII reaction centers and increased non-radiative (heat) dissipation. Optimal F_V/F_M values are ~0.83 (Björkman and Demmig 1987). An increase in F_O indicates PSII inactivation, damage to the oxygen evolving complex and water splitting system, and disruptions in electron donation to PSII reaction centers (Yamashita and Butler 1968, Weis and Berry 1987, Havaux 1996). We did not measure F_O during continuous heating (e.g., Schreiber and Berry 1977) to avoid the confounding effects of previous temperature exposure (e.g., Cunningham and Read 2006, Krause et al. 2010).

Thermotolerance curves derived from electrolyte leakage

During December of 2014, six needles were collected before dawn from each of five seedlings per population and placed in 6 ml of deionized H_2O in 15 ml polycarbonate tubes. Samples were infiltrated under vacuum for 15 min. Tubes were heated for 20 min in a preheated water bath at each of the eight desired temperatures ranging from 30 to 65 °C. Different sets of needles were exposed to each temperature. Tubes were shaken for 1.5 h and the conductivity of the water in each tube was measured with a conductivity meter (Product catalog number 89094–958, VWR International, Radnor, PA, USA). Tubes were then heated for 20 min in a 100 °C water bath and shaken again for 1.5 h. The final conductivity of the solution represented the electrolyte leakage of completely killed leaf tissue. Percent electrolyte leakage or percent damage was calculated as

$$\%\ \text{Electrolyte leakage} = \frac{\text{Conductivity after exposure to temperature (°C)}}{\text{Conductivity after exposure to 100 °C}} \times 100 \quad (2)$$

Growth chamber heat treatment

Seedlings ($N = 7$ per PSME population, $N = 10$ per PIPO population) were exposed to 45 °C for 1 h in a growth chamber (Model I-35LVL, Percival, Boone, IA, USA) with cool white lighting (PPFD = 25 μmol m^{-2} s^{-1}). The treatment temperature of 45 °C was selected based on the chlorophyll fluorescence thermotolerance curves and preliminary experiments at other temperatures that showed that 45 °C induced enough heat stress to be damaging without completely killing needles. This enabled us to evaluate time courses of physiological responses to heat treatment. The treatment temperature is also well above the temperature optimum for photosynthesis between 20 and 30 °C across boreal, temperate and tropical species (Teskey et al. 2015), but realistic for soil surface temperatures experienced during conifer seedling establishment (Kolb and Robberecht 1996). PSME seedlings were heat-treated on 16 October 2014 and PIPO seedlings were heat-treated on 17 November 2014 (see Table S1 available as Supplementary Data at *Tree Physiology* Online). Plants were watered to drainage directly before treatment to avoid drought effects and to buffer changes in soil temperature during treatment. Fine-wire thermocouples measured air, leaf and soil (~10 cm depth) temperatures during treatment exposure (see Table S2 available as Supplementary Data at *Tree Physiology* Online). Pots were completely wrapped with reflective bubble wrap to isolate the soil and roots from heat exposure. This prevented soil temperatures from exceeding 23 °C (see Table S2 available as Supplementary Data at *Tree Physiology* Online), which is realistic for soil temperatures in summer (Zheng et al. 1993, Kolb and Robberecht 1996). Control plants were not exposed to a treatment in the growth chamber. F_V/F_M, photosynthesis, stomatal conductance, foliar carbon isotope ratios and foliar NSC content were monitored in control and treated plants prior to treatment (Day 0) and 1, 2, 7 and 14 days after treatment in five randomly selected plants per treatment group in each population.

Chlorophyll fluorescence, photosynthesis and stomatal conductance

F_V/F_M was measured on five seedlings per treatment group and population at ambient greenhouse temperature with a portable pulse-amplitude modulated chlorophyll fluorometer (Mini-PAM, Heinz Walz Gmbh) at predawn to ensure leaves were dark acclimated. Photosynthesis and stomatal conductance were measured between 10:00 and 13:00 h on five randomly selected seedlings per group and population using a portable photosynthesis system (LI-6400, Li-Cor, Lincoln, NE, USA). In the cuvette, PPFD was set to 1000 μmol m^{-2} s^{-1}, leaf temperature 25 °C, reference [CO_2] 400 μmol mol^{-1} and flow rate 500 μmol s^{-1}. Gas exchange was measured on flattened juvenile needles not in fascicles. Needles were allowed to acclimate to cuvette conditions as long as was required for photosynthesis and conductance levels to stabilize. Needles in the gas exchange chamber were collected and their area was computed using ImageJ software. Measured projected leaf area was used to normalize gas exchange values. Pretreatment (Day 0) photosynthesis values were estimated from photosynthesis-intercellular CO_2 (C_i) curves. To compare intrinsic photosynthesis at the ambient atmospheric CO_2 concentration of 400 μmol mol^{-1}, photosynthesis was estimated at the average C_i value of the control (0 min) group for all sampling days.

Carbon isotope ratios

Five needles from each of five individuals were collected early morning (directly after F_V/F_M measurements were made) on

each sampling date, immediately put on ice in a cooler, and transported to the nearby laboratory where samples were microwaved for 90 s to stop all enzymatic activity because NSC assays were subsequently conducted on aliquots of the same samples. The samples were then oven-dried at 75 °C and stored in a freezer before being ground to a fine powder. Approximately 0.8 mg of dried needle powder was packed in tin capsules for carbon combustion for subsequent analysis by an isotope ratio mass spectrometer. The carbon isotopic ratio ($\delta^{13}C$) was recorded as deviations per mil (‰) from the Vienna Peedee Belemnite international standard. Samples were analyzed for $\delta^{13}C$ at Oregon State University's College of Earth, Oceanic, Atmospheric Sciences stable isotope laboratory. Samples were flash combusted using a Carlo Erba elemental analyzer (NA 1500, Thermo Scientific, Waltham, MA, USA), and the resulting CO_2 was analyzed by a Delta Plus XL continuous-flow mass spectrometer (Finnigan MAT, now Thermo Scientific). Runs were calibrated daily using the international standards USGS40 (glutamic acid) and ANU sucrose. The typical error was ± 0.1‰ or less as determined by repeated measures of internal quality control standards (IAEA-600) and from sample replicates.

The $\delta^{13}C$ of leaf tissue ($\delta^{13}C_{leaf}$) reflects the $\delta^{13}C$ of CO_2 in the atmosphere ($\delta^{13}C_{air}$), the fractionation against the heavier carbon isotope (^{13}C) due to physiological processes and the ratio of the concentration of CO_2 inside the leaf (C_i) to that in the ambient air (C_a):

$$\delta^{13}C_{leaf} = \delta^{13}C_{air} - a - (b - a)\frac{C_i}{C_a} \quad (3)$$

where a is the fractionation effect of diffusion of CO_2 through stomata (4.4‰), and b is the fractionation effect (27‰) associated with discrimination against ^{13}C by the enzyme RUBISCO during carbon fixation (Farquhar et al. 1982, Farquhar and Richards 1984). $\delta^{13}C_{leaf}$ is also an integrated measure of intrinsic water-use efficiency (iWUE) at the time the tissue was formed where greater $\delta^{13}C_{leaf}$ (i.e., less negative) indicates greater iWUE (Farquhar et al. 1989) and drought resistance (Hubick et al. 1986, Jones 2009). Therefore, carbon isotope ratios can indicate ecotypic differences in drought resistance across populations of a species when grown in a common garden situation (Hubick et al. 1986, Zhang et al. 1993, Kerr et al. 2015). Changes in carbon isotope ratios of mature leaves over time can also reflect turnover of NSCs as regulation of photosynthetic gas exchange varies seasonally or following imposition of stress (Gutierrez and Meinzer 1994, Damesin et al. 1998, Scartazza et al. 2013).

Non-structural carbohydrates

The ground needle samples used for $\delta^{13}C$ analyses (described above) were also analyzed for content of total NSC, starch, sucrose and glucose + fructose as described by Woodruff and Meinzer (2011). Water was added to the powdered samples and NSC was extracted from the solutions by heating them in steam for 1.5 h. The concentration of free glucose + fructose was determined photometrically on a 96-well microplate photometer (Multiskan FC, Thermo Scientific) after enzymatic conversion of glucose + fructose to gluconate-6-phosphate. Samples were hydrolyzed by enzymatic treatment: invertase for sucrose and amyloglucosidase for total NSC. Photometric analysis was based on absorbance of samples at 340 nm in solution with reference to the absorbance of a glucose reference solution. Total NSC was calculated as the sum of starch, sucrose and glucose + fructose. NSC values are presented as % dry weight.

Statistics

F_V/F_M values were converted to a percent scale so that the F_V/F_M value of the untreated (control) group was considered 100% (no damage). For ease of comparison with the F_V/F_M thermotolerance curves, the percent electrolyte leakage axis (y-axis) was inverted in figures. Thermotolerance curves assessed with F_V/F_M and electrolyte leakage were determined from third-order sigmoidal functions fitted to the data:

$$f = a/(1 + \exp(-(x - x_0)/b)) \quad (4)$$

where f is the percent of untreated (control) F_V/F_M or percent electrolyte leakage, x is the treatment temperature, and a, x_0 and b are fitting parameters. From this equation, thermotolerance parameters were determined: T_{50} of F_V/F_M is the temperature that caused a 50% reduction in untreated (control) F_V/Fm. T_{50} of electrolyte leakage is the temperature that caused a 50% increase in percent electrolyte leakage or percent damage. The temperature at which F_O begins to rise in response to increasing temperature (T_{crit}) was determined from the intersection of two regression lines extrapolated from the slow- and fast-rising portions of the F_O-temperature curve (Schreiber and Berry 1977). A two-sample t-test was used to compare the T_{50}s assessed from the F_V/F_M and electrolyte leakage methods, and to compare T_{50} and T_{crit} between populations and species.

A three-way factorial linear mixed-effects model was developed with treatment (control, heat), type (species$_{population}$, i.e., PSME$_{dry}$, PSME$_{wet}$, PIPO$_{dry}$ and PIPO$_{wet}$) and day (0, 1, 2, 7 and 14) as fixed main effects. The nested random effect in the model was plant. Response variables were F_V/F_M, photosynthesis, stomatal conductance, $\delta^{13}C$, total NSC, starch, sucrose and glucose + fructose. To choose a correlation structure that would account for the repeated measurements of plants through time, four models that allowed for different residual correlation structures were fit and selected based on the minimum Bayesian information criterion value. Assumptions of constant variance and normality were checked using residual and quantile–quantile plots. Log transformations were necessary to meet assumptions for stomatal conductance, total NSC, starch, sucrose and glucose + fructose. For ease of interpretation, we present back-transformed data in results and figures. All interactive and main effects of factors on

the response were tested using marginal *F*-tests (also known as Type III tests) that account for unbalanced sample sizes. Post hoc comparisons were made using a 95% confidence interval and $P < 0.05$. Due to sufficient degrees of freedom, we did not make multiple comparisons corrections. If no significant differences existed among populations, treatments and/or days, the response variable was pooled by averaging over population, treatment and/or day to simplify data visualization. Statistical analyses were conducted in SigmaPlot 13.0 (Systat Software, San Jose, CA, USA) and R version 3.2.3 (2015-12-10, The R Foundation for Statistical Computing, Vienna, Austria).

Results

Needle thermotolerance curves

Mean ± SE F_V/F_M of untreated, detached needles was 0.72 ± 0.003 for $PIPO_{dry}$, 0.73 ± 0.004 for $PIPO_{wet}$, 0.75 ± 0.006 for $PSME_{dry}$ and 0.74 ± 0.004 for $PSME_{wet}$ and did not significantly differ between populations or species ($P > 0.05$). Thermotolerance curves based on F_V/F_M, electrolyte leakage and F_o showed that PSME was less heat sensitive to temperatures >50 °C than PIPO regardless of population (Figure 1). T_{50} and T_{crit} did not show significant differences between populations but did show significant differences between species where T_{50} (F_V/F_M), T_{50} (electrolyte leakage) and T_{crit} were significantly greater in PSME than PIPO ($P < 0.05$, Table 2).

Whole-plant responses to heat stress

Interactions among the main effects (treatment, type (i.e., $species_{population}$: $PIPO_{dry}$, $PIPO_{wet}$, $PSME_{dry}$, $PSME_{wet}$) and day) on F_V/F_M, photosynthesis, stomatal conductance and $\delta^{13}C$ are summarized in Table 3. F_V/F_M was significantly affected by treatment and day, and the interaction between treatment and day was significant ($P < 0.0001$, Table 3) but the effect of type was not significant ($P = 0.9552$, Table 3). Because there were no significant differences in F_V/F_M, photosynthesis and stomatal conductance between populations within species, populations were pooled (Figure 2). Heat treatment significantly and similarly reduced F_V/F_M 1 and 2 days after treatment in both species (Figure 2a and b). Both species did not recover to pretreatment (Day 0) F_V/F_M values until Day 7. F_V/F_M values of controls did not differ between species.

Photosynthesis was significantly affected by treatment, species and day, and all interactions among main effects were significant ($P < 0.05$, Table 3). Photosynthesis was significantly greater in PIPO than PSME on Days 0, 2 and 7 in controls and on Days 0 and 2 in the heated group (Figure 2c and d). One day after heat treatment, photosynthesis of treated PIPO significantly declined by 81% relative to Day 0 values and became significantly lower than that of treated PSME. Photosynthesis of treated PIPO recovered to control values on Day 14, although photosynthesis on Day 14 was not significantly different from that on Days 2 and 7. In contrast, photosynthesis of the PSME treatment group did not significantly change with day nor differ from the PSME control group.

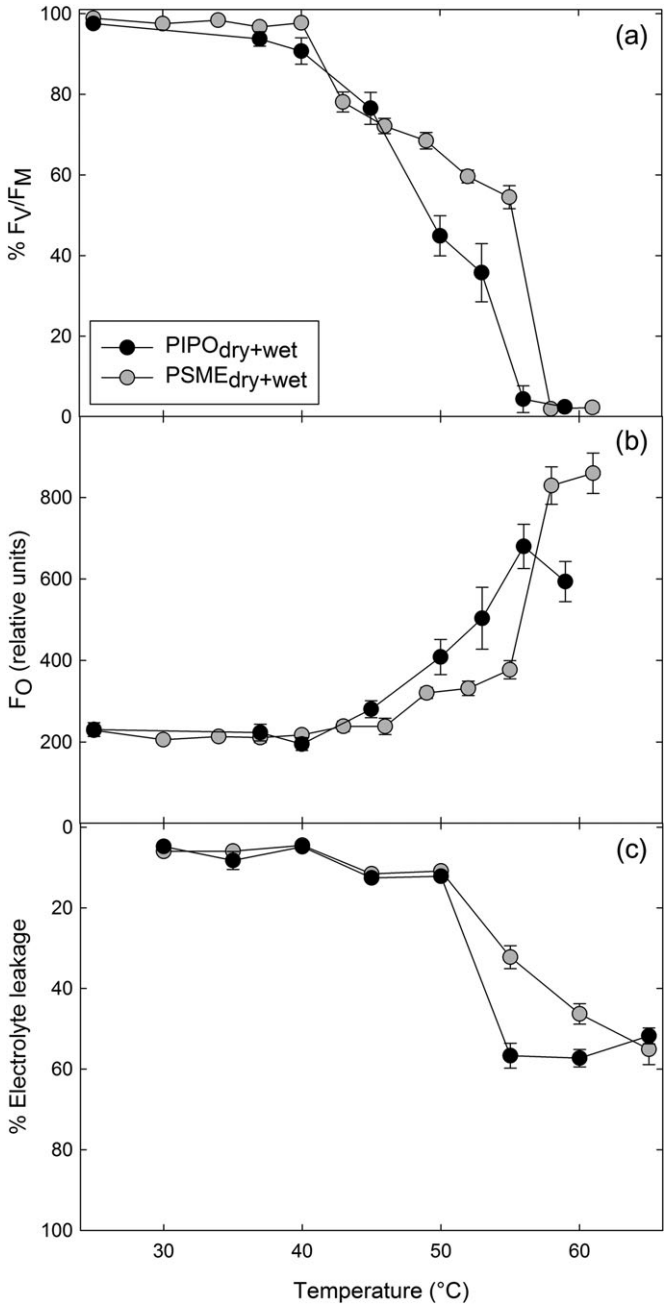

Figure 1. Thermotolerance curves measured with F_V/F_M (a), F_o (b) and electrolyte leakage (c) as a function of temperature for dry, wet and dry + wet populations of PIPO and PSME used to derive thermotolerance parameters: T_{50} (F_V/F_M), T_{50} (electrolyte leakage) and T_{crit} (F_o), respectively. $N = 5$. Error bars represent SE.

Stomatal conductance was significantly affected by species and day ($P < 0.0001$, Table 3), but not treatment ($P = 0.2411$, Table 3). Stomatal conductance of PIPO was significantly greater than PSME on all days in the controls (Figure 2e). This pattern held in the heated group with the only exception on Day 1 after

Table 2. Thermotolerance parameters (°C) derived from curves of F_V/F_M, electrolyte leakage and F_o as a function of treatment temperature for dry, wet and dry + wet populations of PIPO and PSME. Uppercase letters indicate significant differences between species. There were no significant differences between populations. Asterisks indicate significant differences in T_{50} between F_V/F_M and electrolyte leakage methods.

	$PIPO_{dry}$	$PIPO_{wet}$	$PIPO_{dry+wet}$	$PSME_{dry}$	$PSME_{wet}$	$PSME_{dry+wet}$
T_{50} (F_V/F_M)	48.8 ± 1.4*	50.5 ± 0.41*	49.6 ± 0.76 B*	52.8 ± 1.2*	52.0 ± 0.22*	52.4 ± 0.29 A*
T_{50} (electrolyte leakage)	61.8 ± 1.8*	61.6 ± 1.7*	61.7 ± 1.6 B*	63.6 ± 1.5*	66.0 ± 2.4*	64.8 ± 2.3 A*
T_{crit} (F_o)	45.1 ± 0.33	42.3 ± 1.1	44.3 ± 1.0 B	48.1 ± 0.88	48.3 ± 0.30	48.2 ± 0.45 A

$N = 5$. Significance level is at $P < 0.05$. Means ± SE.

treatment when stomatal conductance of treated PIPO significantly declined from Day 0 by 42% and did not differ from that of treated PSME (Figure 2f). In contrast, treated PSME stomatal conductance did not significantly change between Days 0 and 1. Treated PIPO and PSME stomatal conductance changed with day but not in a consistent pattern.

$\delta^{13}C$ was significantly affected by type ($species_{population}$, $P = 0.0157$) and day ($P < 0.0001$), but not treatment ($P = 0.2123$, Table 3). Because $\delta^{13}C$ was not significantly affected by treatment ($P = 0.2123$) and the interaction between day and type was also not significant ($P = 0.3381$), control and treatment $\delta^{13}C$ were pooled for all sampled days in Figure 3. In contrast to all other response variables, $\delta^{13}C$ significantly differed between populations ($P = 0.015$ for PIPO, $P = 0.032$ for PSME) but not between species when populations were pooled ($P = 0.48$, Figure 3). $PSME_{wet}$ and $PIPO_{wet}$ $\delta^{13}C$ values were significantly more negative (i.e., lower) than those of $PSME_{dry}$ and $PIPO_{dry}$ (Figure 3).

Interactions among the main effects (treatment, type and day) on total NSC, starch, sucrose and glucose + fructose are summarized in Table 4. NSC constituents of populations within species did not significantly differ so populations were pooled within species. Total NSC was significantly affected by day ($P = 0.0009$) and marginally by treatment ($P = 0.0465$, Table 4). Total NSC did not differ between species in the control group and only differed between species in the treatment group on Days 7 and 14, and not in a consistent pattern (Figure 4a and b). Starch was significantly affected by day ($P = 0.0001$) and the interaction between treatment and day was significant ($P = 0.0001$). Starch of treated PIPO significantly declined at Day 2 relative to Day 0 before increasing back to pretreatment values at Days 7 and 14 (Figure 4c and d). In contrast, starch of treated PSME steadily declined from Day 0 to Day 14 and was significantly lower than pretreatment values by Day 14. Starch of control PIPO and PSME did not significantly change with day. Sucrose was significantly affected by treatment ($P = 0.0203$), type ($P = 0.0051$), day ($P = 0.002$) and the interaction between treatment and type was significant ($P = 0.0008$). However, sucrose of both PIPO and PSME treatment groups did not significantly differ from that of controls on any day. Sucrose of the heated group only differed between species at Days 1 and 14, and not consistently, while sucrose did not significantly differ between species in the controls (Figure 4e and f). Glucose + fructose was significantly affected by day ($P < 0.0001$) and the interaction between type and day was significant ($P = 0.0033$). Glucose + fructose of both heat-treated PIPO and PSME spiked on Day 2 before declining back to pretreatment values by Day 14 (Figure 4g and h). Control glucose + fructose increased with day in PSME but did not change with day in PIPO. Starch and glucose + fructose of both species were negatively related in the treatment group ($P = 0.049$, $R^2 = 0.40$) but not in the controls (Figure 5).

Discussion

Thermotolerance assessments

Contrary to our hypothesis, PSME had a greater T_{50} assessed with both F_V/F_M and electrolyte leakage and T_{crit} assessed from F_O than PIPO, suggesting that PSME was more heat tolerant than PIPO. This is surprising given the habit of PIPO to establish on sunny, dry sites that experience higher temperatures than the cooler, moister sites on which the relatively more shade-tolerant PSME establishes (Hermann and Lavender 1990, Oliver et al. 1990). This result, however, is consistent with a study on co-occurring field-grown *Pinus halepensis* and *Quercus ilex* where Méthy et al. (1997) also hypothesized that *P. halepensis*, which naturally occurs under warmer and drier conditions and has become more dominant than *Q. ilex* in southern France, would be more heat tolerant than *Q. ilex*. However, the authors found that *P. halepensis* was less heat tolerant than *Q. ilex,* underscoring that leaf heat tolerance is not always directly indicative of a species' distribution pattern and that other life history strategies related to reproductive age, germination rate and dormancy may also impact species' distributions (Méthy et al. 1997). In our study, life history strategies related to seasonal shifts in heat tolerance and rooting may help to elucidate our unexpected results. Heat tolerance of PSME seedlings remains the same year round, whereas that of PIPO has been observed to fluctuate seasonally where heat tolerance declines during dormancy when it becomes fully cold-hardy (Burr et al. 1993). The thermotolerance curves in this study were constructed in October when dormancy of field-grown plants begins, which may be why PIPO appeared to be less heat tolerant than PSME.

Another explanation for the lower heat tolerance in PIPO than PSME may be related to rooting strategies. Unlike PSME, which

Table 3. Marginal *F*-tests for F_V/F_M, photosynthesis, stomatal conductance and $\delta^{13}C$.

	F_V/F_M				Photosynthesis ($\mu mol\ m^{-2}\ s^{-1}$)				Stomatal conductance ($mol\ m^{-2}\ s^{-1}$)				$\delta^{13}C$ (‰)			
	numDF	denDF	*F* value	*P* value	numDF	denDF	*F* value	*P* value	numDF	denDF	*F* value	*P* value	numDF	denDF	*F* value	*P* value
Intercept	1	713	11,530.7	**<0.0001**	1	59	1147.0	**<0.0001**	1	58	3219.2	**<0.0001**	1	48	94,418.91	**<0.0001**
Treatment	1	62	126.8	**<0.0001**	1	58	29.2	**<0.0001**	1	58	1.4	0.2411	1	48	1.60	0.2123
Type ($species_{population}$)	1	62	0.003	0.9552	2	58	12.9	**<0.0001**	2	58	34.5	**<0.0001**	1	48	6.27	**0.0157**
Day	4	713	141.0	**<0.0001**	4	59	12.2	**<0.0001**	4	57	10.0	**<0.0001**	2	37	19.87	**<0.0001**
Treatment x Type	1	62	0.12	0.7322	2	58	4.8	**0.0123**	2	58	0.90	0.4141	1	48	0.25	0.6226
Treatment x Day	4	713	131.6	**<0.0001**	4	59	4.5	**0.0030**	4	57	0.19	0.9451	2	37	4.55	**0.0172**
Type x Day	4	713	0.99	0.4103	8	59	3.6	**0.0017**	8	57	1.5	0.1735	2	37	1.12	0.3381
Treatment x Type x Day	4	713	0.45	0.7692	8	59	2.1	**0.0456**	8	57	1.7	0.1218	2	37	1.85	0.1711

$N = 5$. Bold *P* values indicate $P < 0.05$. Type = $PIPO_{dry}$, $PIPO_{wet}$, $PSME_{dry}$ and $PSME_{wet}$. NumDF and denDF are the degrees of freedom in the numerator and denominator, respectively.

has a relatively shallow root system, PIPO has a deep root system that enables it to access deep soil water and maintain stomatal conductance and evaporative cooling during drought (Kolb and Robberecht 1996, Kerr et al. 2015). This is consistent with the observed greater stomatal conductance in PIPO than PSME (Figure 2). Thus, if grown in the same environment, PSME may experience higher leaf temperatures than does PIPO, which would require a greater heat tolerance in PSME (Cunningham and Read 2006). PIPO seedlings that survived a summer drought in the field used transpiration to maintain leaf and stem temperatures 15 and 30 °C, respectively, further below the surrounding air temperature than those that died (Kolb and Robberecht 1996). Consistent with these findings, PIPO seedlings were less susceptible to drought-induced mortality than PSME seedlings in a common garden experiment (D. Marias, unpublished observations; Rother et al. 2015).

Regardless of population or species, T_{50} measured with electrolyte leakage was significantly greater than T_{50} assessed using F_V/F_M (Table 2, Figure 1), indicating that PSII was more sensitive to heat than cell membranes (Cunningham and Read 2006). This highlights that different plant processes and tissues have different heat tolerances and that overall heat tolerance is difficult to evaluate with one metric (Bilger et al. 1987, Larcher 1995, Schreiber et al. 1995, Teskey et al. 2015).

The mean untreated F_V/F_M range of 0.72–0.75 for both populations and species is lower than optimal values of 0.83 (Björkman and Demmig 1987), which could be related to the low PPFD conditions in the greenhouse. However, the F_V/F_M range is similar to previously reported values for PIPO and PSME in fall and winter, similar to the timing of this experiment (Marshall et al. 2001, Adams et al. 2002). Regardless of population and species, F_V/F_M thermotolerance curves began to significantly decline above ~40 °C (Figure 1a), which is also observed in tropical species (Krause et al. 2010) and is consistent with the finding that optimal leaf temperatures are relatively conserved from subtropical to boreal biomes (Helliker and Richter 2008). F_V/F_M declined to 0 at ~55–58 °C in both species, which is <63 °C, the stem temperature of PIPO seedlings that resulted in mortality (Kolb and Robberecht 1996). This suggests that needle thermotolerance is lower than stem thermotolerance and is consistent with the conclusion that stem temperatures may be a better indicator of seedling mortality than leaf temperatures (Kolb and Robberecht 1996).

Responses to simulated heat wave

Both species exhibited significant reductions in F_V/F_M on Days 1 and 2 after heat treatment (Figure 2), indicating substantial heat-induced damage including impairment of PSII reaction centers and disruptions in electron transport (Maxwell and Johnson 2000, Sharkey 2005, Chen et al. 2012, Zhang et al. 2012). However, heat treatment induced more significant reductions in

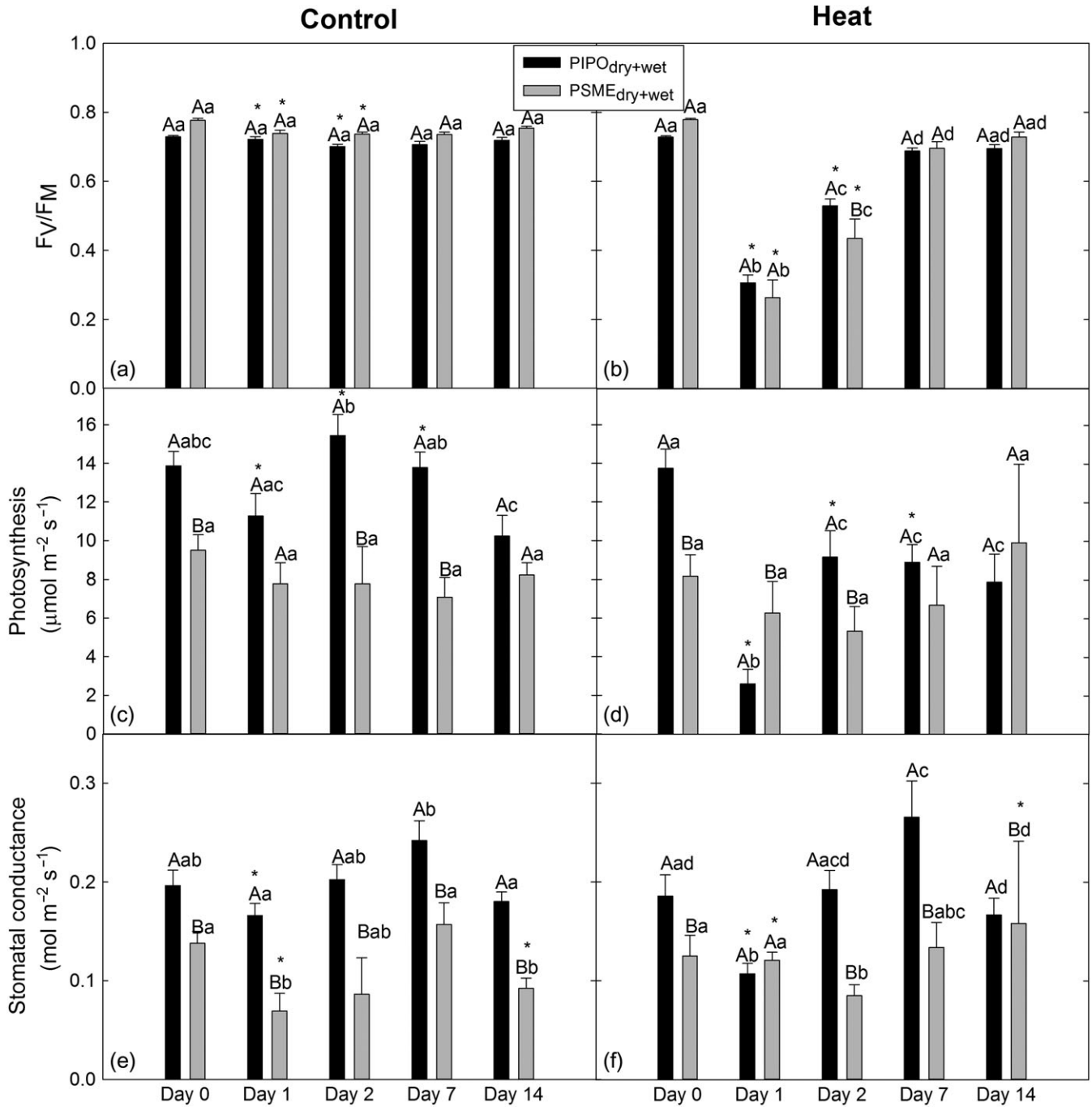

Figure 2. Time courses of mean F_V/F_M (a and b), photosynthesis (c and d), and stomatal conductance (e and f) of PIPO and PSME in control (a, c and e) and heat treatment (b, d and f) groups. Uppercase letters indicate significant differences between species within each day and group. Lowercase letters indicate significant differences among days within species and group. Asterisks indicate significant differences between control and heat treatment groups within species and day. $N = 10$. Error bars represent ± SE.

F_V/F_M than gas exchange in both species (Figure 2). This is consistent with evidence that PSII is the most heat-sensitive component (Havaux 1996) and that reductions in F_V/F_M can occur without corresponding shifts in photosynthesis (Baker 1991, Murchie and Niyogi 2011). Only PIPO displayed a transient reduction in photosynthesis and stomatal conductance 1 day after treatment, which recovered to stable photosynthesis values by Day 2. The transient decline in gas exchange only in PIPO is consistent with the lower T_{50}s, T_{crit} and apparent heat tolerance of PIPO compared with PSME (Table 2, Figure 1) because chlorophyll fluorescence is a proxy for overall photosynthetic performance (Maxwell and Johnson 2000). The greater relative decline in PIPO photosynthesis (81%) than stomatal conductance (42%) indicates that the ratio of photosynthesis to

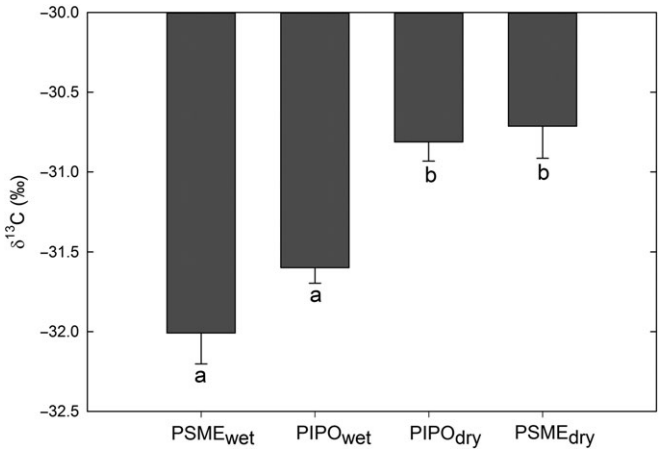

Figure 3. Mean leaf $\delta^{13}C$ of $PIPO_{dry}$, $PIPO_{wet}$, $PSME_{dry}$ and $PSME_{wet}$ pooled for all sampling days and both treatment groups. Letters indicate significant differences among type (i.e., $species_{population}$). Error bars represent ± SE.

stomatal conductance or iWUE (Farquhar et al. 1989) declined after treatment while that of PSME did not change. Although photosynthesis and stomatal conductance are often correlated, the smaller decline in stomatal conductance than photosynthesis in PIPO allowed evaporative cooling to occur when water supply was adequate. This was also observed in loblolly pine (*Pinus taeda*) seedlings in response to a 12 °C heat wave under well-watered conditions (Ameye et al. 2012).

Consistent with previous work, NSC dynamics after heat stress were variable (Sala et al. 2012, Bita and Gerats 2013, Escandón et al. 2016). Although heat treatment did not affect total NSC or sucrose, heat treatment did induce a significant negative relationship between starch and glucose + fructose that was not observed in controls (Figure 5). In PSME from Days 0 to 2, starch declined while glucose + fructose increased, and in PIPO on Day 2, starch was lowest when glucose + fructose was highest (Figures 4 and 5). This may indicate new production of glucose + fructose with concurrent consumption of starch and/or the conversion of starch to glucose + fructose (Geigenberger 2011) in response to heat treatment. Matías et al. (2016) also observed an increase in total soluble sugars in response to elevated temperature in eastern and western provenances of silver fir (*Abies alba* Mill.) seedlings, and Lafta and Lorenzen (1995) found that starch declined in potato leaves in response to heat stress. The lack of treatment effect on sucrose, the end product of photosynthesis, suggests that this pattern was due to the conversion of starch to sugars rather than new production of photosynthate. Consistent with this, leaf $\delta^{13}C$, which can indicate turnover of NSC if $\delta^{13}C$ shifts (Gutierrez and Meinzer 1994, Damesin et al. 1998, Scartazza et al. 2013), was also not affected by treatment. The accumulation of glucose + fructose in response to heat treatment may indicate the allocation of NSC to repairing the heat-induced damage (as indicated by F_V/F_M, Figure 2). Glucose + fructose are necessary for

Table 4. Marginal *F*-tests for total NSC, starch, sucrose and glucose + fructose.

	Total NSC				Starch				Sucrose				Glucose + fructose			
	numDF	denDF	*F* value	*P* value	numDF	denDF	*F* value	*P* value	numDF	denDF	*F* value	*P* value	numDF	denDF	*F* value	*P* value
Intercept	1	97	571.1	**<0.0001**	1	96	14.2	**0.0003**	1	80	472.7	**<0.0001**	1	97	132.7	**<0.0001**
Treatment	1	62	4.1	**0.0465**	1	62	0.11	0.7389	1	62	5.7	**0.0203**	1	62	3.4	0.0699
Type ($species_{population}$)	1	62	1.0	0.3101	1	62	2.1	0.1545	1	62	8.4	**0.0051**	1	62	2.0	0.1583
Day	4	97	5.1	**0.0009**	4	96	7.0	**0.0001**	4	80	6.1	**0.0002**	4	97	8.4	**<0.0001**
Treatment x Type	1	62	1.8	0.1845	1	62	1.7	0.1944	1	62	12.3	**0.0008**	1	62	0.35	0.5581
Treatment x Day	4	97	2.0	0.1041	4	96	6.4	**0.0001**	4	80	0.31	0.8678	4	97	1.1	0.3542
Type x Day	4	97	2.3	0.0688	4	96	1.6	0.1802	4	80	0.43	0.7845	4	97	4.2	**0.0033**
Treatment x Type x Day	4	97	2.7	**0.0374**	4	96	2.4	0.0548	4	80	1.2	0.3294	4	97	0.63	0.6379

$N = 5$. Bold *P* values indicate $P < 0.05$. Type = $PIPO_{dry}$, $PIPO_{wet}$, $PSME_{dry}$ and $PSME_{wet}$. NumDF and denDF are the degrees of freedom in the numerator and denominator, respectively.

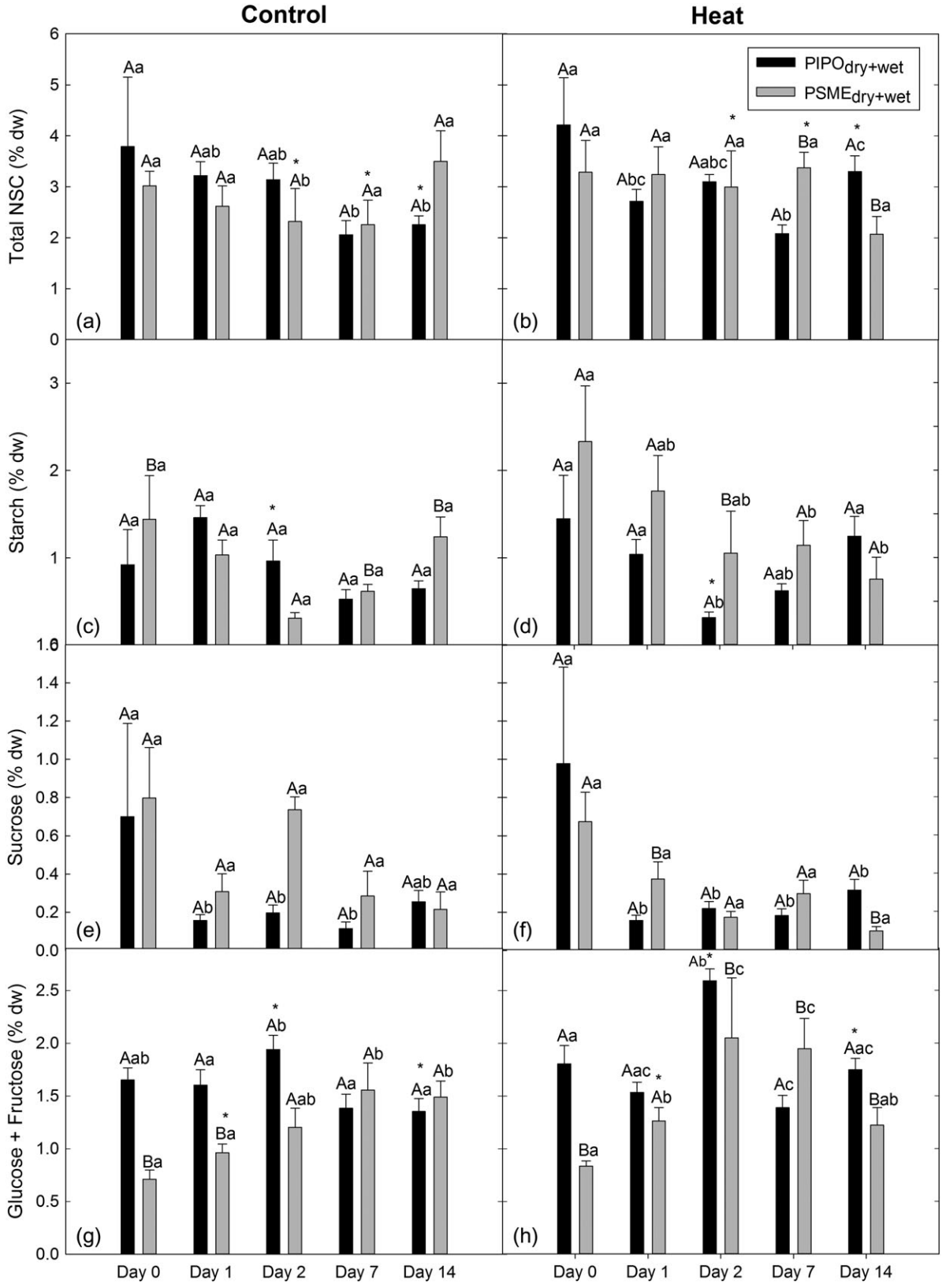

Figure 4. Time courses of mean leaf total NSC (a and b), starch (c and d), sucrose (e and f) and glucose + fructose (g and h) of PIPO and PSME in control (a, c, e, and g) and heat treatment (b, d, f, and h) groups. Uppercase letters indicate significant differences between species within each day and group. Lowercase letters indicate significant differences among days within species and group. Asterisks indicate significant differences between control and heat treatment groups within species and day. $N = 10$. Error bars represent ± SE.

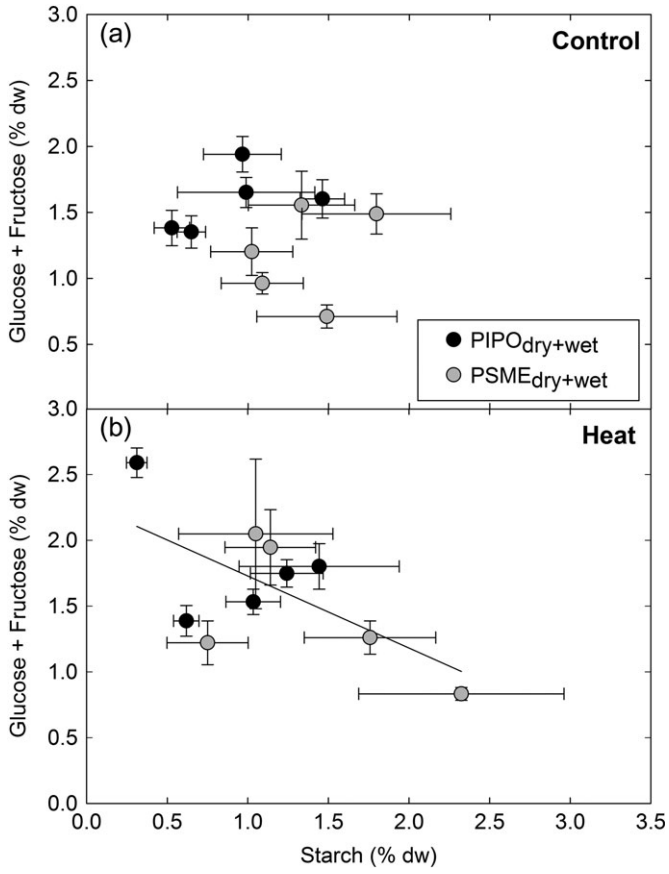

Figure 5. Mean leaf starch plotted against mean glucose + fructose for each sampling day in PIPO and PSME control (a) and heat (b) treatment groups ($R^2 = 0.40$, $P = 0.049$). Error bars represent ± SE.

osmoregulation, maintaining cell water balance and membrane stability (Bita and Gerats 2013), and higher glucose levels have been associated with higher heat stress tolerance (Liu and Huang 2000, Xiong et al. 2015). Although heat-treated PSME demonstrated no shifts in gas exchange, starch of heat-treated PSME steadily declined with day unlike controls (Figure 4c and d). This suggests that heat stress can influence NSC dynamics without changes in gas exchange in PSME. These findings support that the shifts in starch and glucose + fructose (Figure 5) were related to NSC demand (i.e., repair, metabolism) rather than supply (i.e., gas exchange). Although this study was conducted under well-watered conditions, it is likely that high temperature stress will substantially impact carbon metabolism during drought (Adams et al. 2013).

Population differences

We found no significant differences in thermotolerance parameters (e.g., T_{50}, T_{crit}), gas exchange or NSC between populations from different climates of origin (Table 2), consistent with other studies (Maherali et al. 2002, Daas et al. 2008, Gimeno et al. 2009). This may be because our seedlings were grown in and were acclimated to the same environmental growing conditions in the greenhouse. This was also the case in a common garden experiment where coastal and desert species expected to have heat tolerances reflecting the contrasting climates of origin did not display population differences in heat tolerance based on chlorophyll fluorescence (Knight and Ackerly 2002). Similarly, Gimeno et al. (2009) found that the heat tolerance based on chlorophyll fluorescence of *Q. ilex* seedlings increased with increasing exposure to drought and Ghouil et al. (2003) found that T_{crit} increased with greater acclimation temperature independent of climate of origin. Together, these suggest that phenotypic plasticity to the environmental growing conditions may override ecotypic adaptations to the climate of origin (Gimeno et al. 2009) in terms of heat stress responses. However, population differences may become more apparent under greater heat stress (Matías et al. 2016) than that applied in this study.

In contrast to the thermotolerance parameters and heat stress responses, $\delta^{13}C$ significantly differed between populations and reflected each population's climate of origin and associated drought resistance. The $\delta^{13}C$ values were lower than previously reported due to the relatively higher [CO_2] in the greenhouse, common in greenhouse studies (Matías et al. 2016). PIPO$_{dry}$ and PSME$_{dry}$ from climates with lower MAP had greater mean $\delta^{13}C$ than the PIPO$_{wet}$ and PSME$_{wet}$ populations from climates with higher MAP (Table 1, Figure 3). As $\delta^{13}C$ is a proxy for iWUE (Farquhar et al. 1989) and drought resistance (Jones 2009), these data provide support for ecotypic variation in iWUE between populations where populations from drier climates have greater iWUE and drought resistance than those from wetter climates (Schulze et al. 1998, Diefendorf et al. 2010, Kerr et al. 2015). Greater iWUE potentially increases the ratio of carbon gained to water lost through stomata, which becomes increasingly important during drought when plants balance the competing risks of hydraulic failure and impaired carbon assimilation. Thus, populations with greater iWUE are better adapted to cope with drought stress. Although populations differed, $\delta^{13}C$ did not significantly differ between species when populations were pooled. This study was conducted under well-watered conditions but species differences may emerge under drought stress (Matías et al. 2016), given the different drought tolerances and rooting strategies between species. Our results suggest that thermotolerance and heat stress responses may be governed by phenotypic plasticity while drought resistance appeared to be determined by ecotypes and the climate of origin. This may be because the difference in MAP between wet and dry populations was greater than temperature (Table 1).

Conclusions

Due to the projected increases in the frequency of heat waves and drought, the high vulnerability of the seedling developmental stage to heat stress at the soil surface, and the major impacts of

temperature and seedling survival on species' distributions, characterizing seedling physiological responses to heat stress is crucial. This study emphasizes that leaf thermotolerance is only one metric describing how seedlings manage heat stress and that mitigating heat stress involves whole-plant traits and strategies likely including stem thermotolerance, seasonal shifts in thermotolerance and rooting strategies. Heat stress influenced seedling NSC dynamics, providing more evidence that heat stress will impact carbon metabolism during drought. The results also suggest that population differences in drought resistance were driven by climate of origin while heat stress responses were governed more by phenotypic plasticity and acclimation to environmental growing conditions. This is important to consider when predicting responses to future climatic change and identifying physiological mechanisms underpinning shifts in species' distributions.

Supplementary Data

Supplementary data for this article are available at *Tree Physiology* Online.

Acknowledgments

We are grateful to Kelly Kerr and Alicia Magedman for assistance with sowing seeds and the OSU Greenhouse Operations staff for their assistance with the maintenance of plant material.

Funding

This work was supported by the NSF Graduate Research Fellowship Program and NSF grant IOS 11-46746.

Conflict of interest

None declared.

References

Adams HD, Germino MJ, Breshears DD, Barron-Gafford GA, Guardiola-Claramonte M, Zou CB, Huxman TE (2013) Nonstructural leaf carbohydrate dynamics of *Pinus edulis* during drought-induced tree mortality reveal role for carbon metabolism in mortality mechanism. New Phytol 197:1142–1151.

Adams WW III, Demmig-Adams B, Rosenstiel TN, Brightwell AK, Ebbert V (2002) Photosynthesis and photoprotection in overwintering plants. Plant Biol 4:545–557.

Ameye M, Wertin TM, Bauweraerts I, McGuire MA, Teskey RO, Steppe K (2012) The effect of induced heat waves on *Pinus taeda* and *Quercus rubra* seedlings in ambient and elevated CO2 atmospheres. New Phytol 196:448–461.

Aranda I, Alía R, Ortega U, Dantas ÂK, Majada J (2009) Intra-specific variability in biomass partitioning and carbon isotopic discrimination under moderate drought stress in seedlings from four *Pinus pinaster* populations. Tree Genet Genomes 6:169–178.

Baker NR (1991) A possible role for photosystem II in environmental perturbations of photosynthesis. Physiol Plant 81:563–570.

Bilger W, Schreiber U, Lange OL (1987) Chlorophyll fluorescence as an indicator of heat induced limitation of photosynthesis in *Arbutus unedo* L. In: Tenhunen JD, Catarino FM, Lange OL, Oechel WC (eds) Plant response to stress. Springer Berlin Heidelberg:, pp 391–399. http://link.springer.com/chapter/10.1007/978-3-642-70868-8_24 (12 January 2016, date last accessed).

Bita CE, Gerats T (2013) Plant tolerance to high temperature in a changing environment: scientific fundamentals and production of heat stress-tolerant crops. Front Plant Sci 4:273. http://www.ncbi.nlm.nih.gov/pmc/articles/PMC3728475/ (9 February 2016, date last accessed).

Björkman O, Demmig B (1987) Photon yield of O2 evolution and chlorophyll fluorescence characteristics at 77 K among vascular plants of diverse origins. Planta 170:489–504.

Burns, RM, Honkala BH, tech. coords (1990) Silvics of North America: 1. Conifers; 2. Hardwoods. Agriculture Handbook 654. U.S. Department of Agriculture, Forest Service, Washington, DC. vol.2, 877 p.

Burr KE, Wallner SJ, Tinus RW (1993) Heat tolerance, cold hardiness, and bud dormancy relationships in seedlings of selected conifers. J Am Soc Hortic Sci 118:840–844.

Chen WR, Zheng JS, Li YQ, Guo WD (2012) Effects of high temperature on photosynthesis, chlorophyll fluorescence, chloroplast ultrastructure, and antioxidant activities in fingered citron. Russ J Plant Physiol 59:732–740.

Couée I, Sulmon C, Gouesbet G, Amrani AE (2006) Involvement of soluble sugars in reactive oxygen species balance and responses to oxidative stress in plants. J Exp Bot 57:449–459.

Cunningham SC, Read J (2006) Foliar temperature tolerance of temperate and tropical evergreen rain forest trees of Australia. Tree Physiol 26:1435–1443.

Daas C, Montpied P, Hanchi B, Dreyer E (2008) Responses of photosynthesis to high temperatures in oak saplings assessed by chlorophyll-a fluorescence: inter-specific diversity and temperature-induced plasticity. Ann For Sci 65:1.

Damesin C, Rambal S, Joffre R (1998) Seasonal and annual changes in leaf δ13 C in two co-occurring Mediterranean oaks: relations to leaf growth and drought progression. Funct Ecol 12:778–785.

Diefendorf AF, Mueller KE, Wing SL, Koch PL, Freeman KH (2010) Global patterns in leaf 13 C discrimination and implications for studies of past and future climate. Proc Natl Acad Sci USA 107:5738–5743.

Dietze MC, Sala A, Carbone MS, Czimczik CI, Mantooth JA, Richardson AD, Vargas R (2014) Nonstructural carbon in woody plants. Annu Rev Plant Biol 65:667–687.

Du B, Jansen K, Junker LV, Eiblmeier M, Kreuzwieser J, Gessler A, Ensminger I, Rennenberg H (2014) Elevated temperature differently affects foliar nitrogen partitioning in seedlings of diverse Douglas fir provenances. Tree Physiol 34:1090–1101.

Duan H, Amthor JS, Duursma RA, O'Grady AP, Choat B, Tissue DT (2013) Carbon dynamics of eucalypt seedlings exposed to progressive drought in elevated [CO2] and elevated temperature. Tree Physiol 33:779–792.

Escandón M, Cañal MJ, Pascual J, Pinto G, Correia B, Amaral J, Meijón M (2016) Integrated physiological and hormonal profile of heat-induced thermotolerance in *Pinus radiata*. Tree Physiol 36:63–77.

Farquhar G, O'Leary M, Berry J (1982) On the relationship between carbon isotope discrimination and the intercellular carbon dioxide concentration in leaves. Funct Plant Biol 9:121–137.

Farquhar G, Richards R (1984) Isotopic composition of plant carbon correlates with water-use efficiency of wheat genotypes. Funct Plant Biol 11:539–552.

Farquhar GD, Hubick KT, Condon AG, Richards RA (1989) Carbon isotope fractionation and plant water-use efficiency. In: Rundel PW, Ehleringer JR, Nagy KA (eds) Stable isotopes in ecological research. Springer, New York, NY, pp 21–40 http://link.springer.com/chapter/10.1007/978-1-4612-3498-2_2 (11 July 2016, date last accessed).

Geigenberger P (2011) Regulation of starch biosynthesis in response to a fluctuating environment. Plant Physiol 155:1566–1577.

Génard M, Dauzat J, Franck N, Lescourret F, Moitrier N, Vaast P, Vercambre G (2008) Carbon allocation in fruit trees: from theory to modelling. Trees 22:269–282.

Genty B, Briantais J-M, Baker NR (1989) The relationship between the quantum yield of photosynthetic electron transport and quenching of chlorophyll fluorescence. Biochim Biophys Acta 990:87–92.

Ghouil H, Montpied P, Epron D, Ksontini M, Hanchi B, Dreyer E (2003) Thermal optima of photosynthetic functions and thermostability of photochemistry in cork oak seedlings. Tree Physiol 23: 1031–1039.

Gimeno TE, Pías B, Lemos-Filho JP, Valladares F (2009) Plasticity and stress tolerance override local adaptation in the responses of Mediterranean holm oak seedlings to drought and cold. Tree Physiol 29:87–98.

Gutierrez M, Meinzer F (1994) Carbon isotope discrimination and photosynthetic gas exchange in coffee hedgerows during canopy development. Funct Plant Biol 21:207–219.

Hao Z, AghaKouchak A, Phillips TJ (2013) Changes in concurrent monthly precipitation and temperature extremes. Environ Res Lett 8:34014.

Hartmann H, Trumbore S (2016) Understanding the roles of nonstructural carbohydrates in forest trees – from what we can measure to what we want to know. New Phytol 211:386–403.

Havaux M (1996) Short-term responses of Photosystem I to heat stress : induction of a PS II-independent electron transport through PS I fed by stromal components. Photosynth Res 47:85–97.

Helliker BR, Richter SL (2008) Subtropical to boreal convergence of tree-leaf temperatures. Nature 454:511–514.

Hermann RK, Lavender DP (1990) Silvics of Douglas-fir. In: Burns R.M., Honkala B.H., tech. coords (eds) Silvics of North America, Volume 1, Conifers. Agric. Handbk. 654. Forest Service, U.S. Department of Agriculture, Washington, DC, pp 413–424.

Horváth I, Glatz A, Nakamoto H, Mishkind ML, Munnik T, Saidi Y, Goloubinoff P, Harwood JL, Vigh L (2012) Heat shock response in photosynthetic organisms: membrane and lipid connections. Prog Lipid Res 51:208–220.

Hubick K, Farquhar G, Shorter R (1986) Correlation between water-use efficiency and carbon isotope discrimination in diverse peanut (*Arachis*) germplasm. Aust J Plant Physiol 13:803.

Intergovernmental Panel on Climate Change (2014) Synthesis Report. Contribution of Working Groups I, II and III to the Fifth Assessment Report of the Intergovernmental Panel on Climate Change [Core Writing Team, Pachauri RK, Meyer LA (eds)]. IPCC, Geneva, Switzerland, 151 pp.

Jones HG (2009) What is water use efficiency? In: Bacon M (ed) Water use efficiency in plant biology. Blackwell Publishing, Oxford, pp 27–41.

Kerr KL, Meinzer FC, McCulloh KA, Woodruff DR, Marias DE (2015) Expression of functional traits during seedling establishment in two populations of *Pinus ponderosa* from contrasting climates. Tree Physiol 35:535–548.

Knight CA, Ackerly DD (2002) An ecological and evolutionary analysis of photosynthetic thermotolerance using the temperature-dependent increase in fluorescence. Oecologia 130:505–514.

Kolb PF, Robberecht R (1996) High temperature and drought stress effects on survival of *Pinus ponderosa* seedlings. Tree Physiol 16:665–672.

Kozlowski T (1992) Carbohydrate sources and sinks in woody plants. Bot Rev 58:107–222.

Krause GH, Winter K, Krause B, Jahns P, García M, Aranda J, Virgo A (2010) High-temperature tolerance of a tropical tree, *Ficus insipida*: methodological reassessment and climate change considerations. Funct Plant Biol 37:890–900.

Lafta AM, Lorenzen JH (1995) Effect of high temperature on plant growth and carbohydrate metabolism in potato. Plant Physiol 109:637–643.

Larcher W (1995) Photosynthesis as a tool for indicating temperature stress events. In: Schulze PDE-D, Caldwell PDMM (eds) Ecophysiology of photosynthesis. Springer, Berlin Heidelberg, pp 261–277. http://link.springer.com/chapter/10.1007/978-3-642-79354-7_13 (10 February 2016, date last accessed).

Lindgren K, Hällgren J-E (1993) Cold acclimation of *Pinus contorta* and *Pinus sylvestris* assessed by chlorophyll fluorescence. Tree Physiol 13:97–106.

Liu X, Huang B (2000) Carbohydrate accumulation in relation to heat stress tolerance in two creeping bentgrass cultivars. J Am Soc Hortic Sci 125:442–447.

Maherali H, Williams BL, Paige KN, Delucia EH (2002) Hydraulic differentiation of Ponderosa pine populations along a climate gradient is not associated with ecotypic divergence. Funct Ecol 16:510–521.

Marshall JD, Rehfeldt GE, Monserud RA (2001) Family differences in height growth and photosynthetic traits in three conifers. Tree Physiol 21:727–734.

Matías L, Gonzalez-Díaz P, Quero JL, Camarero JJ, Lloret F, Jump AS (2016) Role of geographical provenance in the response of silver fir seedlings to experimental warming and drought. Tree Physiol. 36:1236–1246.

Maxwell K, Johnson GN (2000) Chlorophyll fluorescence—a practical guide. J Exp Bot 51:659–668.

Méthy M, Gillon D, Houssard C (1997) Temperature-induced changes of photosystem II activity in *Quercus ilex* and *Pinus halepensis*. Can J For Res 27:31–38.

Murchie EH, Niyogi KK (2011) Manipulation of photoprotection to improve plant photosynthesis. Plant Physiol 155:86–92.

Niinemets Ü (2010) Responses of forest trees to single and multiple environmental stresses from seedlings to mature plants: past stress history, stress interactions, tolerance and acclimation. For Ecol Manage 260:1623–1639.

Oliver WW, Ryker RA (1990) Silvics of ponderosa pine. In: Burns R.M., Honkala B.H., tech. coords (eds) Silvics of North America, Volume 1, Conifers. Agric. Handbk. 654. Forest Service, U.S. Department of Agriculture, Washington, DC, pp 413–424.

Perić S, JAZBEC A, Tijardović M, Margaletić J, Ivanković M, Pilaš I, Medak J (2009) Provenance studies of Douglas fir in the locality of "Kontija" (Istria). Period Biol 111:487–493.

Ramírez-Valiente JA, Sánchez-Gómez D, Aranda I, Valladares F (2010) Phenotypic plasticity and local adaptation in leaf ecophysiological traits of 13 contrasting cork oak populations under different water availabilities. Tree Physiol 30:618–627.

Roitsch T, González M-C (2004) Function and regulation of plant invertases: sweet sensations. Trends Plant Sci 9:606–613.

Rother MT, Veblen TT, Furman LG (2015) A field experiment informs expected patterns of conifer regeneration after disturbance under changing climate conditions. Can J For Res 45:1607–1616.

Sala A, Woodruff DR, Meinzer FC (2012) Carbon dynamics in trees: feast or famine? Tree Physiol 32:764–775.

Salvucci ME, Crafts-Brandner SJ (2004) Relationship between the heat tolerance of photosynthesis and the thermal stability of rubisco activase in plants from contrasting thermal environments. Plant Physiol 134:1460–1470.

Scartazza A, Moscatello S, Matteucci G, Battistelli A, Brugnoli E (2013) Seasonal and inter-annual dynamics of growth, non-structural carbohydrates and C stable isotopes in a Mediterranean beech forest. Tree Physiol 33:730–742.

Schreiber U, Berry JA (1977) Heat-induced changes of chlorophyll fluorescence in intact leaves correlated with damage of the photosynthetic apparatus. Planta 136:233–238.

Schreiber U, Bilger W, Neubauer C (1995) Chlorophyll fluorescence as a nonintrusive indicator for rapid assessment of in vivo photosynthesis. In: Schulze PDE-D, Caldwell PDMM (eds) Ecophysiology of photosynthesis. Springer, Berlin Heidelberg, pp 49–70. http://link.springer.com/chapter/10.1007/978-3-642-79354-7_3 (10 February 2016, date last accessed).

Schulze E-D, Williams RJ, Farquhar GD, Schulze W, Langridge J, Miller JM, Walker BH (1998) Carbon and nitrogen isotope discrimination and nitrogen nutrition of trees along a rainfall gradient in northern Australia. Funct Plant Biol 25:413–425.

Sevanto S, Dickman LT (2015) Where does the carbon go? Plant carbon allocation under climate change. Tree Physiol 35:581–584.

Sharkey TD (2005) Effects of moderate heat stress on photosynthesis: importance of thylakoid reactions, rubisco deactivation, reactive oxygen species, and thermotolerance provided by isoprene. Plant Cell Environ 28:269–277.

Sorensen FC (1983) Geographic variation in seedling Douglas-Fir (*Pseudotsuga Menziesii*) from the Western Siskiyou Mountains of Oregon. Ecology 64:696–702.

Sugio A, Dreos R, Aparicio F, Maule AJ (2009) The cytosolic protein response as a subcomponent of the wider heat shock response in Arabidopsis. Plant Cell 21:642–654.

Teskey R, Wertin T, Bauweraerts I, Ameye M, McGuire MA, Steppe K (2015) Responses of tree species to heat waves and extreme heat events. Plant Cell Environ 38:1699–1712.

Tomlinson KW, Poorter L, Sterck FJ, Borghetti F, Ward D, de Bie S, van Langevelde F (2013) Leaf adaptations of evergreen and deciduous trees of semi-arid and humid savannas on three continents. J Ecol 101:430–440.

Wahid A, Gelani S, Ashraf M, Foolad MR (2007) Heat tolerance in plants: an overview. Environ Exp Bot 61:199–223.

Weis E, Berry JA (1987) Quantum efficiency of photosystem II in relation to 'energy'-dependent quenching of chlorophyll fluorescence. Biochim Biophys Acta 894:198–208.

Woodruff DR, Meinzer FC (2011) Water stress, shoot growth and storage of non-structural carbohydrates along a tree height gradient in a tall conifer. Plant Cell Environ 34:1920–1930.

Xiong D, Yu T, Ling X, Fahad S, Peng S, Li Y, Huang J (2015) Sufficient leaf transpiration and nonstructural carbohydrates are beneficial for high-temperature tolerance in three rice (*Oryza sativa*) cultivars and two nitrogen treatments. Funct Plant Biol 42:347–356.

Yamashita T, Butler WL (1968) Photoreduction and photophosphorylation with tris-washed chloroplasts. Plant Physiol 43:1978–1986.

Zhang J, Marshall JD, Jaquish BC (1993) Genetic differentiation in carbon isotope discrimination and gas exchange in *Pseudotsuga menziesii*. Oecologia 93:80–87.

Zhang J-L, Poorter L, Hao G-Y, Cao K-F (2012) Photosynthetic thermotolerance of woody savanna species in China is correlated with leaf life span. Ann Bot 110:1027–1033.

Zhao J, Hartmann H, Trumbore S, Ziegler W, Zhang Y (2013) High temperature causes negative whole-plant carbon balance under mild drought. New Phytol 200:330–339.

Zheng D, Hunt ER Jr, Running SW (1993) A daily soil temperature model based on air temperature and precipitation for continental applications. Clim Res 2:183–191.